ПИ
980/S2S

Volume 217 September 2014 ISSN 0022-4596

ELSEVIER

JOURNAL OF SOLID STATE CHEMISTRY

Editor
M.G. KANATZIDIS

Associate Editors
S.J. HWANG
J. LI
S.J. CLARKE
H.-C. ZUR LOYE

IN THIS ISSUE:

Structural, magnetic, and oxygen storage properties of hexagonal $Dy_{1-x}Y_xMnO_{3+\delta}$

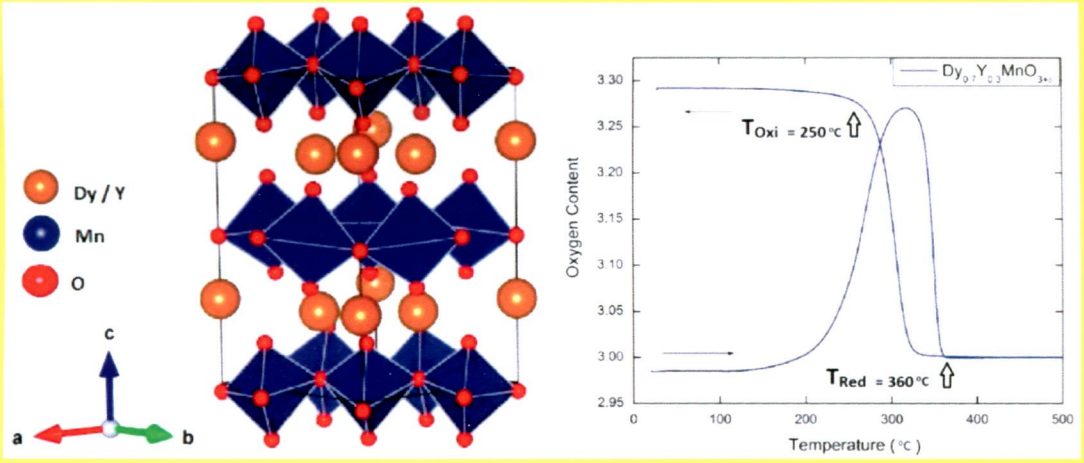

C. Abughayada, B. Dabrowski, M. Avdeev, S. Kolesnik, S. Remsen and O. Chmaissem

Available online at www.sciencedirect.com

ScienceDirect

ELSEVIER

Volume 217, September 2014

CONTENTS

JOURNAL OF SOLID STATE CHEMISTRY

www.elsevier.com/locate/jssc

Abstracted/indexed in BioEngineering Abstracts, Chemical Abstracts, Coal Abstracts, Current Contents/Physics, Chemical, & Earth Sciences, Engineering Index, Research Alert, SCISEARCH, Science Abstracts, and Science Citation Index. Also covered in the abstract and citation database SCOPUS®. Full text available on ScienceDirect®.

Regular Articles

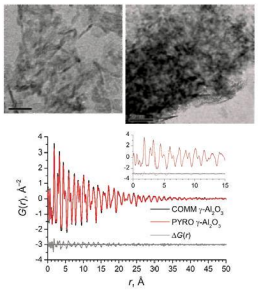

Boehmite-derived and sol–gel synthesized porous γ-Al_2O_3 possess identical structural properties, featuring a nm scale local structure and a tetragonal average structure.

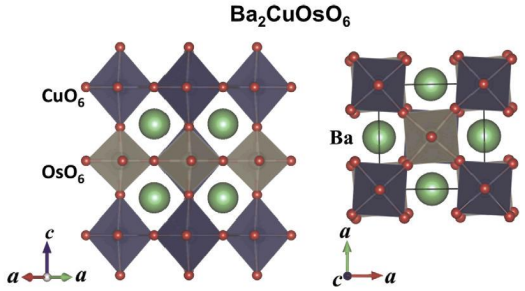

A new compositional double perovskite oxide Ba_2CuOsO_6 synthesized by a high-pressure (6 GPa) and high-temperature (1500 °C) method.

Regular Articles—Continued

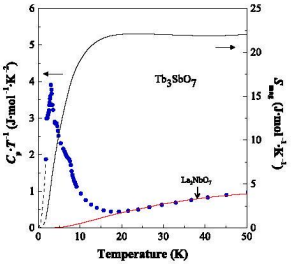

Temperature dependence of the specific heat divided by temperature (C_p/T) and the magnetic entropy (S_{mag}) for Tb_3SbO_7. Two-step magnetic transition has been observed.

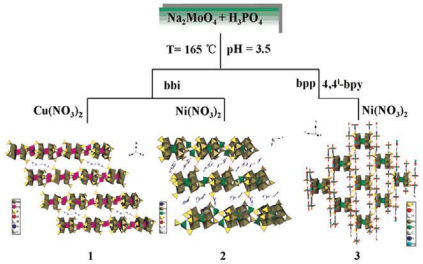

As new linking unit, $Cu(H_2O)_3$, $Ni(H_2O)$, and $\{Ni_2(H_2O)_{10}Na(PCA)_2\}$ are introduced into $\{TM(P_4Mo_6)_2\}$ reaction systems to assemble three supramolecular materials under hydrothermal conditions via changing organic ligand and transition metal.

Continued

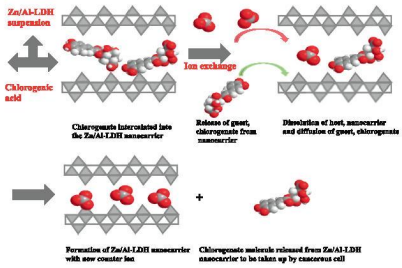

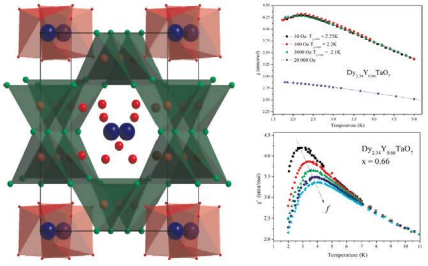

Weberite-type crystal structure of the $Dy_{3-x}Y_xTaO_7$ compounds. In this structure the magnetic sublattice is formed by Dy^{3+} cations in an arrangement of distorted tetrahedra at the second-nearest neighbor site; this arrangement suggests geometric frustration that leads to a spin glass behavior

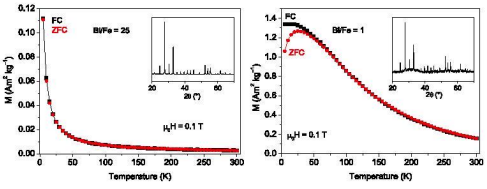

$Bi_{25}FeO_{40}$ powders were prepared by a hydrothermal method and a combustion process. The optical band gaps and the peritectic point were determined. The magnetic behaviour was investigated depending on the synthesis and the initial Bi/Fe ratios. The influence of amorphous iron-oxide on the magnetic properties was examined.

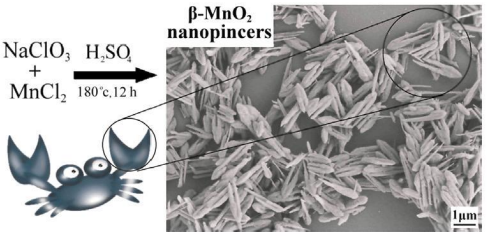

Branched β-MnO_2 bipods with novel nanopincer morphology were prepared by a facile one-pot hydrothermal method through oxidizing $MnSO_4$ with $NaClO_3$ in H_2SO_4 condition without using any surfactants or templates.

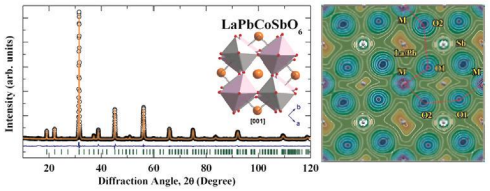

XRD Rietveld refinement result of $LaPbCoSbO_6$ presented a large BO_6 octahedral distortion along the *ab* plane. Based upon the variations from Co–O–Sb bond angles, a fierce competition from many extended magnetic coupling routes (*M*–O–O–*M*) would induce a considerably large magnetic frustration and electron hopping restriction.

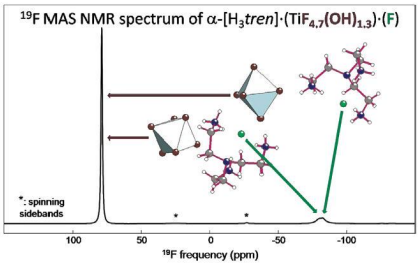

The ratio of the relative intensities of the ^{19}F NMR lines assigned to F atoms belonging to isolated $TiF_{6-x}(OH)_x$ octahedra and to "free" fluoride ions shows that the F^-/OH^- substitution concerns only F atoms bonded to titanium.

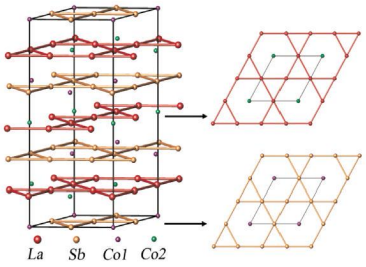

$La_3Sb_3Co_2O_{14}$ crystallizes in a pyrochlore related structure with an ordered distribution of cations, giving rise to two sets of ideal 2D Kagome lattices formed by La^{3+} or Sb^{3+} respectively. This rhombohedral pyrochlore is a tolerant structure for stable compounds composed by many light rare-earth and *d*-transition elements. Substituting Zn^{2+} or Mg^{2+} for Co^{2+} will provide a series of compounds useful for studying magnetic interactions in the rare-earth Kagome lattices.

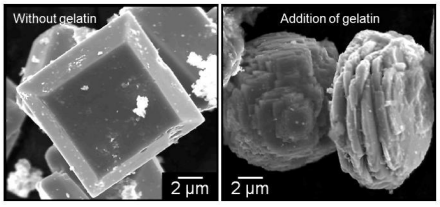

Nanostructured SnO particles were obtained from $Sn_6O_4(OH)_4$ by the hydrothermal treatment in gelatin solutions.

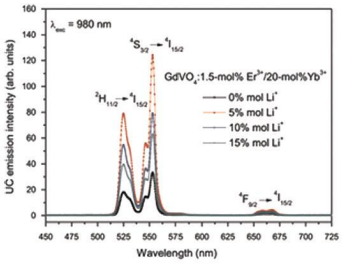

UC emission spectra for $GdVO_4$:1.5-mol% Er^{3+}/20-mol% Yb^{3+} powders co-doped with different concentrations of Li^+ ions, recorded under 980-nm excitation.

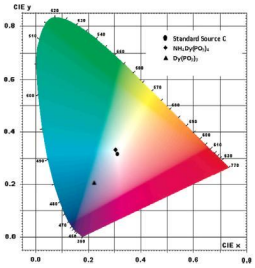

The CIE color coordinate diagrams showing the chromatic coordinates of Dy^{3+} luminescence in $NH_4Dy(PO_3)_4$ and $Dy(PO_3)_3$.

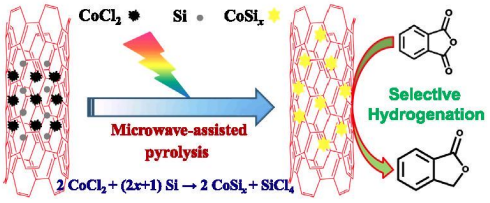

$CoSi_x$/CNTs catalysts with different $CoSi_x$ phases ($CoSi_2$, CoSi) have been rapidly synthesized via microwave-assisted route, which involves the vaporization of $CoCl_2$ and subsequent reaction of $CoCl_2$ with Si.

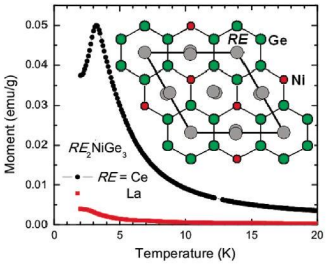

The compounds La_2NiGe_3 and Ce_2NiGe_3 crystallize in the Er_2RhSi_3 type. Magnetic susceptibility show antiferromagnetic ordering for Ce_2NiGe_3 at 3.2 K and neutron diffraction confirms the absence of long range ordering.

Continued

Effect of an electric field on the properties of BN Möbius stripes

J. Lemos de Melo, S. Azevedo and J.R. Kaschny

page 120

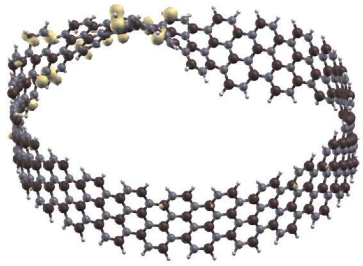

Calcium substitution in rare-earth metal germanides with the hexagonal Mn_5Si_3 structure type. structural characterization of the extended series $RE_{5-x}Ca_xGe_3$ (*RE*=Rare-earth metal)

Nian-Tzu Suen, Matthew Broda and Svilen Bobev

page 142

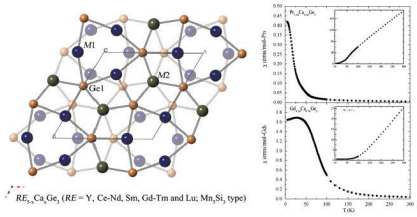

The family of rare-earth metal–calcium–germanides with the general formula $RE_{5-x}Ca_xGe_3$ (*RE*=Y, Ce–Nd, Sm, Gd–Tm and Lu) crystallize in the hexagonal space group $P6_3/mcm$ (No. 193, Pearson symbol *hP*16) with a structure that is a variant of the Mn_5Si_3 structure type.

Structural, magnetic, and oxygen storage properties of hexagonal $Dy_{1-x}Y_xMnO_{3+\delta}$

C. Abughayada, B. Dabrowski, M. Avdeev, S. Kolesnik, S. Remsen and O. Chmaissem

page 127

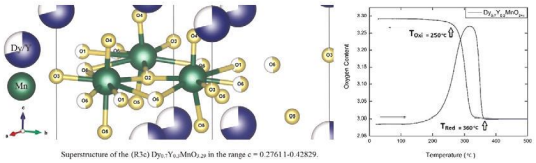

Superstructure of the ($R3c$) $Dy_{0.7}Y_{0.3}MnO_{3.29}$ in the lattice range c=0.27611–0.42829 (left panel) along with its low-temperature oxygen absorption/desorption capability in pure O_2 (right panel).

New MOF based on lithium tetrahydrofuran-2,3,4,5-tetracarboxylate: Its structure and conductivity behavior

Vitezslav Zima, Deepak S. Patil, Duraisamy Senthil Raja, Ting-Guang Chang, Chia-Her Lin, Koichi Shimakawa and Tomas Wagner

page 150

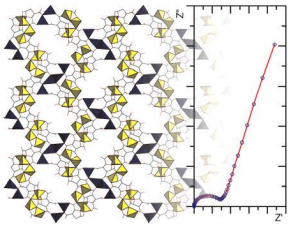

Structure of a new metal organic framework was determined and its ionic conductivity was evaluated using a random-walk approach.

Long persistent and optically stimulated luminescence behaviors of calcium aluminates with different trap filling processes

Buhao Zhang, Xuhui Xu, Qianyue Li, Yumei Wu, Jianbei Qiu and Xue Yu

page 136

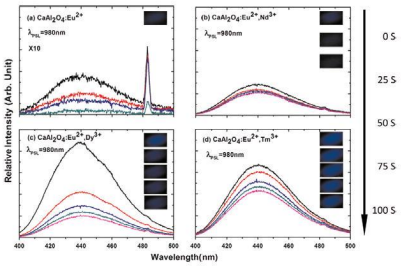

OSL emission spectra of $Ca_{0.995}Al_2O_4$:0.0025Eu^{2+}, 0.0025R^{3+} (*R*=Nd, Dy, Tm) taken under varying stimulation time (0, 25, 50, 75, 100 s). Inset: Blue emission pictures under varying stimulation time.

Self-irradiation and oxidation effects on americium sesquioxide and Raman spectroscopy studies of americium oxides

Denis Horlait, Richard Caraballo, Florent Lebreton, Christophe Jégou, Pascal Roussel and Thibaud Delahaye

page 159

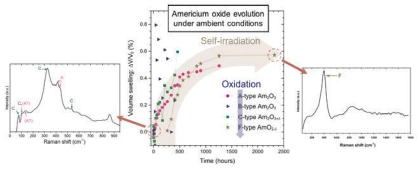

The evolution of americium oxide under ambient conditions was monitored using XRD (X-ray diffraction) and Raman spectroscopy. After a thermal treatment under reducing conditions, a polyphasic sample mainly composed of A- and C-type americium sesquioxides is evidenced by XRD and Raman spectroscopy. The sample then evolves through two processes: oxidation and self-irradiation. The first one provokes the progressive appearance of F-type americium dioxide while the initial phases disappear, whereas the main effect of the second is a structural swelling with time.

Clathrate formation in the systems Sr–Cu–Ge and {Ba,Sr}–Cu–Ge

I. Zeiringer, R. Moser, F. Kneidinger, R. Podloucky, E. Royanian, A. Grytsiv, E. Bauer, G. Giester, M. Falmbigl and P. Rogl

page 169

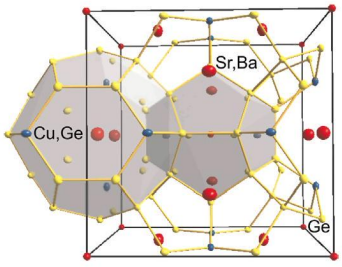

Clathrate type-I unit cell including the coordination polyhedra for the Sr (or Ba) atoms.

The structures and properties of the new two-dimensional inorganic–organic hybrid materials based on the molybdate chains

Na Li, Bao Mu, Xinyu Cao and Rudan Huang

page 180

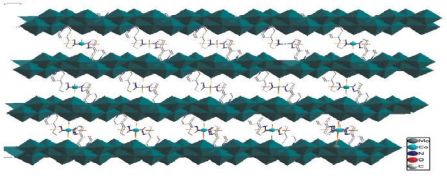

In complex **1**, The Co ion is six coordinated by four oxygen atoms from two Mo_6O_{20} and two water molecules, and two N atoms from two different ligand. It is noticeable that there is an one-dimensional chain molybdate, which is combined by O–Mo–O, then the chain parallel with each other, the Mo_6 anion acts as a bidentate ligand providing O7 atoms to bridge CoII ions to form a 2D inorganic layer. Finally every nets become 3D structure by hydrogen bond.

Language services. Authors who require information about language editing and copyediting services pre- and post-submission please visit http://www.elsevier.com/locate/languagepolishing or our customer support site at http://epsupport.elsevier.com. Please note Elsevier neither endorses nor takes responsibility for any products, goods or services offered by outside vendors through our services or in any advertising. For more information please refer to our Terms & Conditions http://www.elsevier.com/termsandconditions

For a full and complete Guide for Authors, please go to: http://www.elsevier.com/locate/jssc

Journal of Solid State Chemistry has no page charges.